Commun. Comput. Phys.
doi: 10.4208/cicp.220113.090813a

Vol. **15**, No. 3, pp. 756-775
March 2014

Numerical Simulation of Unidirectional Stratified Flow by Moving Particle Semi Implicit Method

Shaoshan Rong[1], Haiwang Li[1,2], Martin Skote[1], Teck Neng Wong[1,*] and Fei Duan[1]

[1] *School of Mechanical and Aerospace Engineering, Nanyang Technological University, 50 Nanyang Avenue, Singapore 639798.*
[2] *National Key Lab of Science and Technology on Aero-Engines, Beijing University of Aeronautics and Astronautics, Beijing 100191, China.*

Received 22 January 2013; Accepted (in revised version) 9 August 13

Available online 3 December 2013

Abstract. Numerical simulation of stratified flow of two fluids between two infinite parallel plates using the Moving Particle Semi-implicit (MPS) method is presented. The developing process from entrance to fully development flow is captured. In the simulation, the computational domain is represented by various types of particles. Governing equations are described based on particles and their interactions. Grids are not necessary in any calculation steps of the simulation. The particle number density is implicitly required to be constant to satisfy incompressibility. The weight function is used to describe the interaction between different particles. The particle is considered to constitute the free interface if the particle number density is below a set point. Results for various combinations of density, viscosity, mass flow rates, and distance between the two parallel plates are presented. The proposed procedure is validated using the derived exact solution and the earlier numerical results from the Level-Set method. Furthermore, the evolution of the interface in the developing region is captured and compares well with the derived exact solutions in the developed region.

AMS subject classifications: 76TXX

Key words: Moving particle semi-implicit, liquid-liquid stratified flow, flow developing.

1 Introduction

Stratified two-phase flow is commonly found in petroleum and chemical processing industries where crude oil and water are produced from wells and transported in a pipeline [1–3]. Therefore, it is necessary to understand the flow behavior phenomena of

*Corresponding author. *Email addresses:* 19820912@sina.com (S. Rong), liha0008@e.ntu.edu.sg (H. Li), MSKOTE@ntu.edu.sg (M. Skote), mtnwong@ntu.edu.sg (T. N. Wong), FeiDuan@ntu.edu.sg (F. Duan)

liquid-liquid systems. In particular, prediction of the flow characteristics, such as velocity distribution, pressure gradient, and holdup of liquid, are essential for proper design of two-phase flow systems, and have been predicted and measured since the 1930s.

Many empirical correlations based on different flow conditions were developed experimentally. Chenais and Hulin [4] measured water holdup in a 20cm-diameter pipe at mean velocities between 2.7 and 3.5cm/s. The pressure gradient of the liquid-liquid co-current flow in 2.54cm pipes was measured by Angeli and Hewitt [5]. Abduvyat et al. [6] measured pressure drop and liquid holdup of liquid-liquid flow in a horizontal pipe with 4 inch diameter. Some researchers also conducted experimental studies on liquid-liquid systems in various pipes [7–10]. However, the prediction capabilities are generally restricted to the flow conditions on which they are based.

Mathematical modeling provides another method to study the liquid-liquid flow system. Most of previous methods describing the liquid-liquid flow were based on empirical correction such as the correction proposed by Lockhart and Martinelli [11]. In a general case, analytical solution was limited to solving a laminar-laminar two-phase stratified flow based on different interface geometry. The other researchers [12–16] solved the fully developed Navier-Stokes equations and obtained exact solutions which were expressed in the terms of Fourier series or Fourier integrals with constant interface geometry. Brauner et al. [14] developed another model to improve the understanding of laminar-laminar two-phase flow. Hall and Hewitt [17] developed an analytical model to predict liquid-liquid laminar flow in a circular pipe. The exact solutions about holdup of liquid dependent on Martenelli parameter as well as viscosity ratio of the two phases were obtained. For complex problems, such as turbulent-turbulent liquid-liquid flow, accurate solutions can be obtained numerically. Torres-Monzon [3] introduced a two-dimensional model for fully developed, turbulent-turbulent liquid-liquid stratified flow. The velocity profiles of both phases showed an agreement with the experimental data.

Most of the analytical and semi-empirical models can predict and describe the fully developed conditions of two-phase flow. Computational fluid dynamic (CFD) plays an important role in understanding the physics in two-phase flows. Compared with experimental and analytical methods, CFD is simpler, faster and more economical. Khor et al. [18] numerically studied one-dimensional modeling to predict the phase holdups and developed a computer code. Elseth et al. [19] simulated the turbulent stratified liquid-liquid pipe flow using a Volume of Fluid (VOF) model. However, their numerical results cannot compare well with experimental data. Gao et al. [1] improved Elseth's VOF model to compute turbulent smooth-stratified liquid-liquid flow in a horizontal pipe. Surface tension is included in Gao's paper. Yap et al. [20] developed models for uniform stratified flow of two liquids using the Level-Set method. A significant advantage of the level set method is that it may be combined very effectively with anisotropic mesh adaptivity to get very efficient solutions [21, 22]. Razwan [2] numerically simulated stratified liquid-liquid two-phase flow using multiphase volume of fluid model. The velocity distribution and holdup of liquids were compared with experimental data.

The interfacial interaction is a critical factor to predict the flow behavior [23]. The

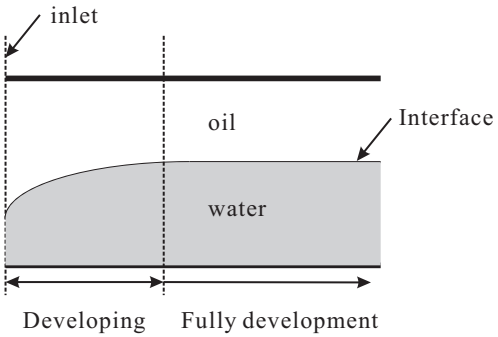

Figure 1: Liquid-liquid two-phase stratified flow.

flow patterns of two-phase flow is defined according to different interface shape [24,25]. Most of the previous works cannot adequately account for interfacial interaction between two phases. For the Level-Set and VOF methods, the interface was captured within the flow field computation by solving a special equation on Eulerian grid. In 1996, a new method called Moving Particle Semi-implicit (MPS) method for incompressible flow was proposed by Koshizuka and Oka [26]. Compared with Level-Set and VOF methods, MPS can track the fluid flow and interface deformation simultaneously without introducing any extra equations and special treatments for the interface. This method avoids mesh generation and numerical diffusion due to the fully Lagrangian treatment of discrete particles. This method has been explained and reviewed by Gotoh and Sakai [27].

This article presents a MPS method to simulate liquid-liquid two-phase stratified flow between two parallel plates. The flow behavior from the inlet to the fully development is simulated. Fig. 1 illustrates the problem. Unlike the Level-Set method and VOF method, the MPS method is based on different types of particles and their interactions. To complement the numerical simulations, an analytical method is presented for the prediction of the fully developed flow. The analysis focuses on steady-state solutions of the continuity and momentum equations.

The substance of this article is divided into three sections. The governing equations, the MPS method and the numerical procedure are discussed in the next section. Analytical solution is in Section 3. This is followed by the analysis of the results in section four. Finally, some conclusions are given.

2 Mathematical formulation

2.1 The theory about MPS method

The MPS method was first proposed by Koshizuka and Oka in 1996 [6]. It uses different types of particles to represent different parts of the computational domain. In the frame work of this method, particles contain the information of flow velocity, pressure and density. Each particle interacts with all neighbor particles in the vicinity of a kernel. The

information about each particle can be evaluated by the information and weight function of neighboring particles. Finally, the governing equations change into the particle interaction model. The Navier-Stokes equation is then discretized into the particle interaction equation based on a particle interaction model. Incompressibility is calculated by a semi-implicit algorithm where the pressure field is implicitly solved using the Poisson equation, while the other terms are explicitly calculated.

2.2 Governing equations

In this paper, two liquid are assumed to be incompressible liquid. Governing equations for an incompressible liquid are expressed by the conservation laws of mass and momentum

$$\frac{D\rho}{Dt}=0 \tag{2.1}$$

and

$$\frac{D\mathbf{u}}{Dt}=-\frac{1}{\rho}\nabla p+\nu\nabla^2\mathbf{u}+\mathbf{g}, \tag{2.2}$$

where $D=\frac{\partial}{\partial t}+\mathbf{u}\cdot\nabla$, ρ denotes the density, t the time, p the pressure, $\mathbf{u}$ the velocity, ν the kinematic viscosity, and $\mathbf{g}$ the gravity acceleration. In the MPS method presented in this paper, the term of $\frac{D\rho}{Dt}$ and $\frac{D\mathbf{u}}{Dt}$ are directly expressed by calculating moving particles.

In MPS method, the density of liquids, ρ in Eq. (2.1) and Eq. (2.2) is expressed using the mass of the particle and the number density of the particle

$$\rho_i=(m\rho)_i=\frac{m_i n_i}{\oint_{\mathrm{v}_i} w(r)d\mathrm{v}} \tag{2.3}$$

and

$$n_i=\sum_{j\neq i} w\big(|\mathbf{r}_j-\mathbf{r}_i|\big). \tag{2.4}$$

In Eqs. (2.3) and (2.4), ρ_n is the number density of the particle, the subscript i and j means the arbitrary different particles respectively, m denotes mass of a particle, n is the particle number density, $|\mathbf{r}|$ is the magnitude of vector $\mathbf{r}$, v_i is the maximum incidence of the weight function for particle i. For incompressible flow, the fluid density is required to be constant. The constant value of the particle number density is denoted by n^0. In the present investigation, as multiple materials of different densities are calculated simultaneously, the particle mass is changed and the particle number density n^0 is kept constant. The term $w(r)$ represents a weight function which measures the interaction between a particle and its neighboring particles. The weight function is defined as

$$w(r)=\begin{cases}\dfrac{r_e}{r}-1, & 0\leq r<r_e,\\ 0, & r_e<r,\end{cases} \tag{2.5}$$

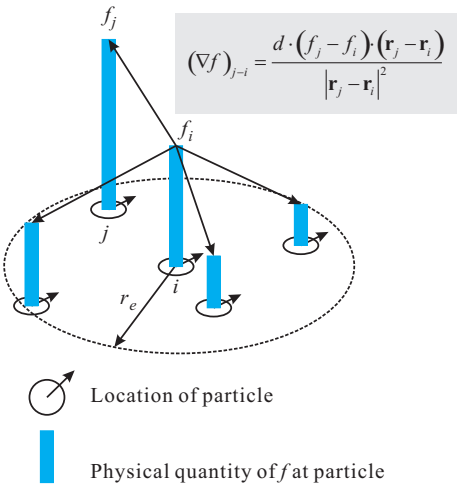

Figure 2: The concept of gradient model.

where r_e is a finite distance which restricts the interaction, r denotes the distance between the particle and the neighboring particles. Eq. (2.5) indicates that it is infinity at $r=0$. $r_e = 2l_0$ is used in this paper. This is good for avoiding clustering of particles, which is explained by Koshizuka et al. [28].

The governing equations of Eqs. (2.1) and (2.2) include the gradient operator and the Laplacian operator. These operators can be expressed using the weight function. A gradient vector between two neighboring particles i and j can be described as (Appendix A)

$$(\nabla f)_{j-i} = \frac{d(f_j - f_i)(\mathbf{r}_j - \mathbf{r}_i)}{|\mathbf{r}_j - \mathbf{r}_i|^2}, \tag{2.6}$$

where f is arbitrary physical quantity, d is the number of space dimensions. In this paper, $d=2$. The gradient vector at $\mathbf{r}_i$ is the weight average effect of all neighboring particles. According the definition of Eq. (2.6), the gradient vector at $\mathbf{r}_i$ can be described as (Fig. 2)

$$(\nabla f)_i = \frac{d}{n^0}\sum_{j\neq i}\left[\frac{f_j - f_i^*}{|\mathbf{r}_j - \mathbf{r}_i|^2}(\mathbf{r}_j - \mathbf{r}_i)w(|\mathbf{r}_j - \mathbf{r}_i|)\right]. \tag{2.7}$$

Comparing Eq. (2.6) and Eq. (2.7), the equations indicate that f_i in Eq. (2.6) is replaced by f_i^* in Eq. (2.7). f_i^* is determined by the following equation

$$f_i^* = \min(f_j) \quad \text{for} \quad \{j | w(|\mathbf{r}_j - \mathbf{r}_i|) \neq 0\}. \tag{2.8}$$

This method was suggested by Koshizuka et al. [28]. It is beneficial for the numerical stability.

The Laplacian operator is modeled based on the understanding about transient diffusion problems. Part of a quantity retained by a particle i will diffuse to neighboring

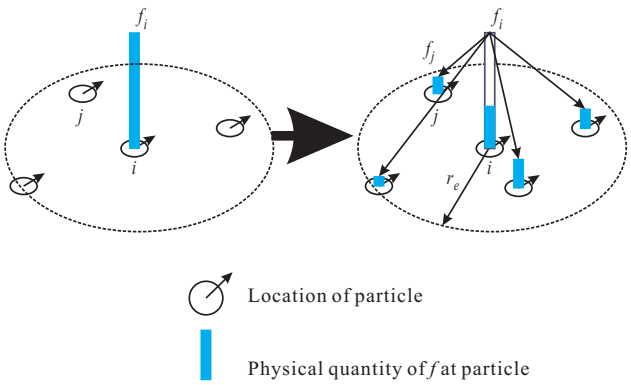

Figure 3: Concept of Laplacian model.

particles j. The quantity diffused from i to j can be calculated using the weight function (Fig. 3)

$$\Delta f_{i-j}=\frac{2d\nu\Delta t}{n^0\lambda}f_i w(|\mathbf{r}_j-\mathbf{r}_i|), \tag{2.9}$$

where λ can be described as

$$\lambda=\frac{\sum_{j\neq i}w(|\mathbf{r}_j-\mathbf{r}_i|)|\mathbf{r}_j-\mathbf{r}_i|^2}{\sum_{j\neq i}w(|\mathbf{r}_j-\mathbf{r}_i|)}. \tag{2.10}$$

Based on Eqs. (2.9) and (2.10), the Laplacian operator of particle i can be expressed as (Appendix B)

$$(\nabla^2 f)_i=\frac{2d}{n^o\lambda}\sum_{j\neq i}(f_j-f_i)w(|\mathbf{r}_j-\mathbf{r}_i|). \tag{2.11}$$

Substituting Eqs. (2.3), (2.7) and (2.11) into Eq. (2.2), the discrete formation of governing equation Eq. (2.2) can be expressed as (Appendix C)

$$\begin{aligned}&\frac{mn}{\oint_{V_i}w(r)d\mathrm{v}}\frac{\mathbf{u}}{\Delta t}+\mathbf{u}\frac{d}{n^0}\sum_{j\neq i}\left[\frac{\mathbf{u}_j-\mathbf{u}_i}{|\mathbf{r}_j-\mathbf{r}_i|^2}(\mathbf{r}_j-\mathbf{r}_i)w(|\mathbf{r}_j-\mathbf{r}_i|)\right]\\&=-\nabla p+\frac{\mu_i 2d}{n^o\lambda}\sum_{j\neq i}(\mathbf{u}_j-\mathbf{u}_i)w(|\mathbf{r}_j-\mathbf{r}_i|).\end{aligned} \tag{2.12}$$

For an incompressible liquid, the particle number density is constant and equal to n^0. In the calculation, the new particle number density is assumed as n^*. In the iteration, the calculated new particle number density (n^*) is not equal to the constant value n^0. In order to keep the particle number density constant and equal to n^0, the deviation of the particle number density (n') is calculated as

$$n'=n^0-n^*. \tag{2.13}$$

Substituting Eqs. (2.3) and (2.13) into the continuity equation of Eq. (2.1), it is expressed as

$$n' = -(\Delta t) n^0 (\nabla \cdot \mathbf{u}'). \tag{2.14}$$

The modification of the velocity $\mathbf{u}'$ can be calculated from the pressure gradient according the simplified MAC (SMAC) method [29]:

$$\mathbf{u}'|^s = -\frac{\Delta t}{\rho} \nabla p|^{s+1}, \tag{2.15}$$

where $f|^s$ is the calculated value of f in step s of the iteration. Substituting Eqs. (2.14) and (2.15) into Eq. (2.13), the Poisson equation of pressure is expressed as (Appendix D)

$$(\nabla^2 p|^{s+1})_i = -\frac{\rho}{(\Delta t)^2} \frac{(n^*)_i - n^o}{n^o}. \tag{2.16}$$

Combining Eqs. (2.11) and (2.12) with Eq. (2.16) together, the discrete formation of governing equation for the iteration s can be described as

$$\begin{aligned} &\frac{mn}{\oint_{\mathrm{v}_i} w(r) d\mathrm{v}} \frac{\mathbf{u}_i|^s}{\Delta t} + \mathbf{u}_i|^s \frac{d}{n^0} \sum_{j \neq i} \left[\frac{\mathbf{u}_j|^s - \mathbf{u}_i|^s}{|(\mathbf{r}_j|^s - \mathbf{r}_i|^s)|} (\mathbf{r}_j|^s - \mathbf{r}_i|^s) w(|(\mathbf{r}_j|^s - \mathbf{r}_i|^s)|) \right] \\ =&\frac{d}{n^0} \left\{ \sum_{j \neq i} \left[\frac{2\mu_i}{\lambda} (\mathbf{u}'_j|^s - \mathbf{u}'_i|^s) - \frac{(p_j|^s - p_i^*|^s)}{|(\mathbf{r}_j|^s - \mathbf{r}_i|^s)|} (\mathbf{r}_j|^s - \mathbf{r}_i|^s) \right] w(|(\mathbf{r}_j|^s - r_{\mathbf{i}}|^s)|) \right\} \end{aligned} \tag{2.17}$$

and

$$\frac{2d}{n^o \lambda} \sum_{j \neq i} (p_j|^s - p_i|^{s+1}) w((\mathbf{r}_j|^s - \mathbf{r}_i|^s)) = -\frac{1}{(\Delta t)^2} \frac{m_i \mathbf{u}'_i|^s}{\int w(|(\mathbf{r}_j|^s - \mathbf{r}_i|^s)|) dv}. \tag{2.18}$$

2.3 Boundary conditions

Boundary conditions in this paper include free surface boundary conditions and rigid wall boundary conditions.

In MPS method, particle number density is used to determine the free surface. Since no particle exists in the outside of the free surface, the particle number density is low at particles on the free surface. Thus, a particle is considered on the surface if it satisfies

$$\langle n \rangle_i^* < \beta n^o, \tag{2.19}$$

where β is a parameter. Almost the same solution was obtained between $\beta = 0.8$ and $\beta = 0.99$. Following the references [26, 28], $\beta = 0.95$ is chosen in this paper. A Dirichlet boundary condition of pressure is given to this particle.

The rigid wall boundary is represented by arranging fixed wall particles, which is much simpler than the corresponding procedure for grid methods. The particles are divided into two parts: particle within the fluids and particle within the wall. When the pressure is calculated, the particles within the fluid layer contacting with the wall are involved while the particles within the wall are not included. It means that the particles within the wall have no effect on the pressure calculation. When the velocity is calculated, velocity of particle within the liquid was updated according the calculation. But the velocities of particle within the wall are always zero.

2.4 Summary of the solution

The solution procedure is described in Fig. 4. It can be summarized as follows:

(1) Give the initial information of all particles. The initial information of all particles includes velocity of particle, location of particle, and pressure at the location of the particle.

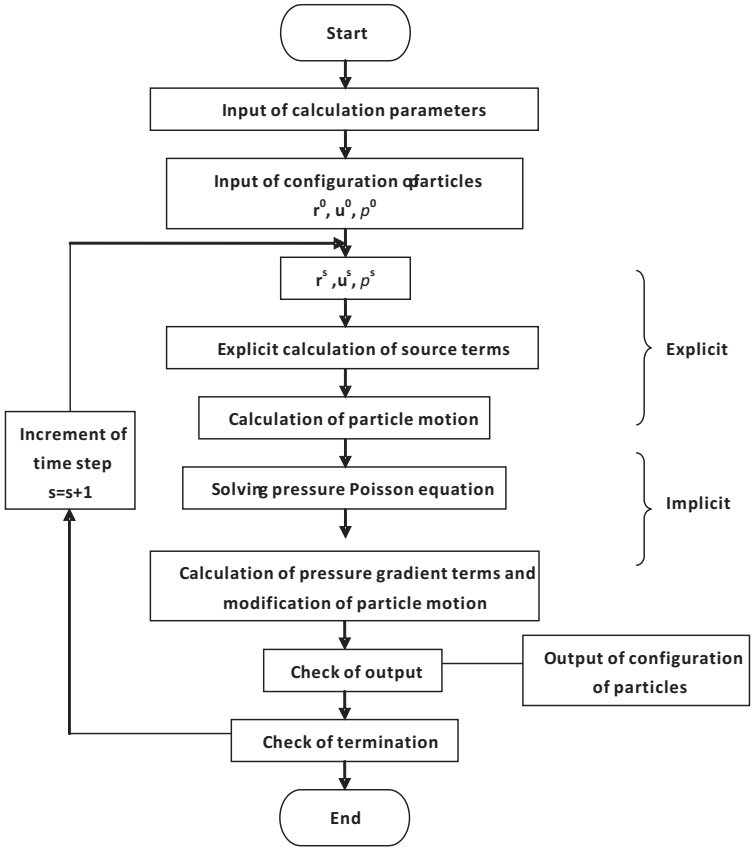

Figure 4: The algorithm of the simulation program using MPS methods.

(2) Solve the governing equation (2.18) to calculate the new pressure $p_i|^{s+1}$.

(3) Submit new pressure $p_i|^{s+1}$ into Eq. (2.17) to calculate new velocity $\mathbf{u}_i|^{s+1}$.

(4) Calculate particle motion according $\mathbf{r}_i|^{s+1}=\mathbf{r}_i|^s+(\Delta t)\mathbf{u}_i|^{s+1}$.

(5) Update the value of velocity, location of particle, and pressure according the values of $\mathbf{u}_i|^{s+1}$, $\mathbf{r}_i|^{s+1}$, and $p_i|^{s+1}$.

(6) Repeat steps from 2 to 5 until the solution converges.

3 Analytical solution for liquid-liquid flow between parallel plates for fully developed steady flow

The movement of liquids can be described using Eq. (2.2). For the fully developed liquid-liquid flow, Eq. (2.2) reduces as

$$\nabla^2\mathbf{u}=\frac{1}{\mu}\nabla p. \tag{3.1}$$

The boundary conditions at the wall is

$$u_1(0)=0, \tag{3.2a}$$
$$u_2(1)=0. \tag{3.2b}$$

The velocity and the shear stress at the interface $(y=h)$ is continuous

$$-\frac{1}{\mu_1}\frac{dp}{dx}h^2+A_1h=-\frac{1}{\mu_2}\frac{dp}{dx}h^2+A_2h+\frac{1}{\mu_2}\frac{dp}{dx}-A_2. \tag{3.3}$$

The shear stress is also continuous at the interface

$$\mu_1\left(\frac{\partial u_1}{\partial y}\right)_h=\mu_2\left(\frac{\partial u_2}{\partial y}\right)_h. \tag{3.4}$$

Substituting boundary conditions (Eqs. (3.2a)-(3.4)) into governing equations, the velocity profiles can be described as

$$u_1=-\frac{1}{2}\frac{1}{\mu_1}\frac{dp}{dx}y^2+A_1y+B_1, \tag{3.5a}$$
$$u_2=-\frac{1}{2}\frac{1}{\mu_2}\frac{dp}{dx}y^2+A_2y+B_2, \tag{3.5b}$$

where

$$A_1=\frac{2Q_1}{h^2}-\frac{4Q_2h\left(\frac{\mu_2}{\mu_1}h-h+1\right)}{(1-h)^2\left(h^2-\frac{\mu_1}{\mu_2}h^2+2\frac{\mu_1}{\mu_2}h-\frac{\mu_1}{\mu_2}-4h\right)}, \tag{3.6a}$$

$$A_2=-\frac{2Q_2}{(1-h)^2}-\frac{4Q_2(h+2)\left(h-h\frac{\mu_1}{\mu_2}+\frac{\mu_1}{\mu_2}\right)}{(1-h)^2\left(h^2-\frac{\mu_1}{\mu_2}h^2+2\frac{\mu_1}{\mu_2}h-\frac{\mu_1}{\mu_2}-4h\right)}, \tag{3.6b}$$

$$B_1=0, \tag{3.6c}$$

$$B_2=\frac{1}{\mu_2}\frac{dp}{dx}-A_2, \tag{3.6d}$$

$$\frac{dp}{dx}=-\frac{6Q_2\mu_2\left(h-h\frac{\mu_1}{\mu_2}+\frac{\mu_1}{\mu_2}\right)}{(1-h)^2\left(h^2-\frac{\mu_1}{\mu_2}h^2+2\frac{\mu_1}{\mu_2}h-\frac{\mu_1}{\mu_2}-4h\right)}, \tag{3.6e}$$

Q_1 and Q_2 are the total flow rates of liquid 1 and liquid 2, respectively. The interface location (h) can be calculated according the continuity condition of velocity at the interface by iterating the following equation:

$$\frac{Q_1}{Q_2}\frac{\mu_1}{\mu_2}\frac{(1-h)^2}{h^2}\left(h^2-\frac{\mu_1}{\mu_2}h^2+2\frac{\mu_1}{\mu_2}h-\frac{\mu_1}{\mu_2}-4h\right)+\left(h^2-\frac{\mu_1}{\mu_2}h^2-2h\frac{\mu_1}{\mu_2}+3\frac{\mu_1}{\mu_2}\right)=0. \tag{3.7}$$

4 Results and discussion

Fig. 1 describes the overall configuration of the developing processing of the liquid-liquid two-phase flow. For given inlet velocities or flow rates, the code of this paper with MPS method simulates the development of velocity and interface locations. Three problems are considered:

(1) Various particle densities were used in order to determine the suitable particle density for the simulation. This procedure corresponds to grid independency check for a conventional CFD method. In this problem, two liquids have equal properties including density, viscosity, and inlet velocity. The initial height keeps the constant values of $h_{1,inlet}=0.3$W and $h_{2,inlet}=0.7$W where W is the distance between two parallel plates. In this paper, W is 100μm. This problem determines the suitable particle density in the following calculations.

(2) The proprieties of two liquids (including density and viscosity) also set to equal values. The volumetric flow rates are consistent. In the calculation, the inlet heights ($h_{1,inlet}$ and $h_{2,inlet}$) changes.

(3) The mass flow rate, density, and viscosity of two liquids have different values.

The second problem and the third problem indicate the capabilities of the procedure of capturing the interface position.

4.1 Validation of MPS method

In this part, for the channel geometry, the length is set to $L=500\mu$m and the width is $W=100\mu$m. Two immiscible fluids with the same density ($\rho_1=\rho_2=\rho$) and viscosities ($\mu_1=\mu_2=\mu$) are considered. With this choice of properties, the velocity profile of two-phase flow is in fact the single-phase flow velocity. To initiate this study, the inlet velocities of the two fluids are also set to the same value, $u_{1,inlet}=u_{2,inlet}=1$cm/s. The inlet interface location is $h_{1,inlet}=0.3$W and $h_{2,inlet}=0.7$W. For the number of particle in the computational domain, computations are carried out using 1.25×10^4, 1.5×10^4, 1.75×10^4, 2×10^4, and 2.25×10^4. It can be seen in Fig. 5 that the interface location does not change when 2×10^4 and 2.25×10^4 are used. As a result, unless otherwise specified, 2×10^4 is used as particle number in the subsequence computations. It is obvious that from Fig. 5 that there is no noticeable change in the interface location beyond $x/\mathrm{W}=0.8$ with the interface setting down at around $h_{1,inlet}=0.3$W. This indicates that the flow becomes fully developed at $x/\mathrm{W}=0.8$.

The efficiency of algorithm for the MPS method is calculated. Fig. 6 indicated the results. For the number of particle in the computational domain, computations are carried out using 1.25×10^4, 1.5×10^4, 1.75×10^4, 2×10^4, and 2.25×10^4. The computational time increases dramatically as the increase of particle number. With the same computational accuracy, one case using the MPS method (2.25×10^4) need about 48 hours but it needs more than 60 hours using the Level set method.

Fig. 7 shows the interface location and the velocity profiles at three streamwise locations. The inlet condition and liquid properties are set to be same with Fig. 5. The velocity profiles and interface locations are compared with results calculated using Level-Set method [20]. The fully developed velocity profile and interface location also compare

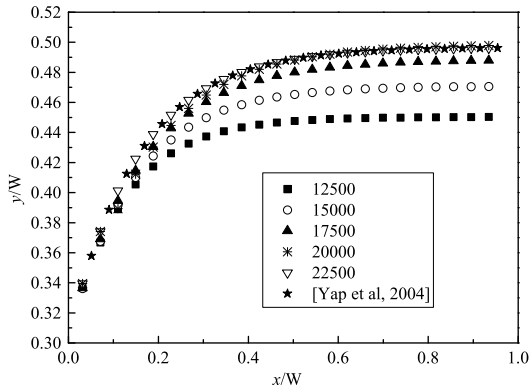

Figure 5: Particle number independent study for the interface location when two liquids have identical properties.

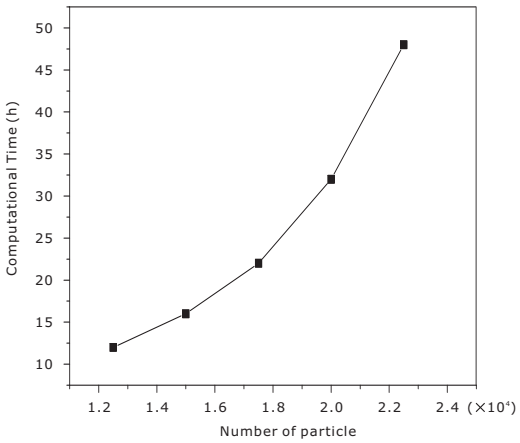

Figure 6: The efficiency of the algorithm with various particle number.

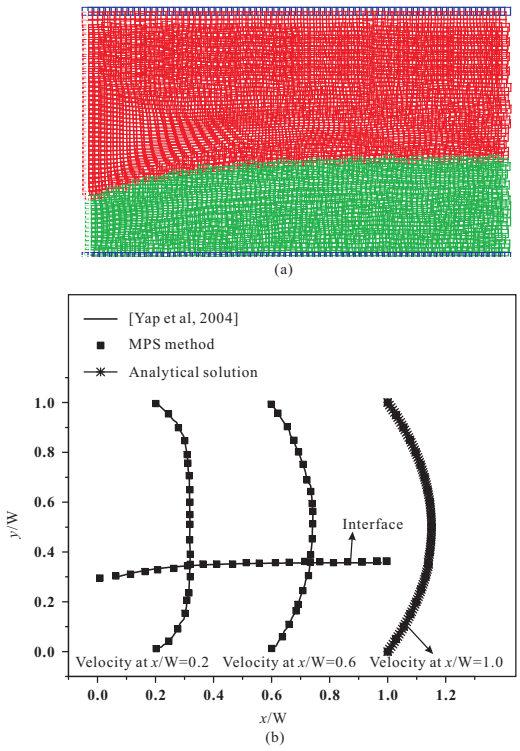

Figure 7: Evolutions of velocity and interface profiles along flow directions for $h_{1in}/W=0.3$, $\mu_1=\mu_2$, $\rho_1=\rho_2$, $\mathbf{u}_1=\mathbf{u}_2$: (a) MPS results; (b) Comparison of MPS results with published Level-Set method [20] and analytical solutions.

with analytical solution of Eqs. (3.5a) and (3.5b). The results using MPS method is identical to the published data and exact solutions. This shows that with MPS method, the velocity profile and interface are correctly captured.

4.2 Liquid-liquid flow with different properties

Fig. 8 shows the evolutions of the interface for three values of the inlet heights $(h_{1,\text{inlet}})$, namely, $h_{1,inlet}=0.3$W, $h_{1,inlet}=0.5$W, $h_{1,inlet}=0.7$W, respectively. In this problem, the two liquids has same properties $(\rho_1=\rho_2=\rho,\ \mu_1=\mu_2=\mu)$. The volumetric flow rates are identical $(Q_1=Q_2)$. A channel with the length $L=500\mu$m and the width $W=100\mu$m is studied. The figure shows that the interface evolves along the axial direction. It also indicates that for fully developed flow, the interfaces with different inlet height are developed to $h=0.5$. This indicates that the fully developed interface location is dependent on the volumetric flow rates but is independent of the inlet height, $h_{1,inlet}$.

The evolutions of the velocity and the interface location for two liquids with different inlet velocity and viscosity are shown in Fig. 9. In this figure, the inlet height of water

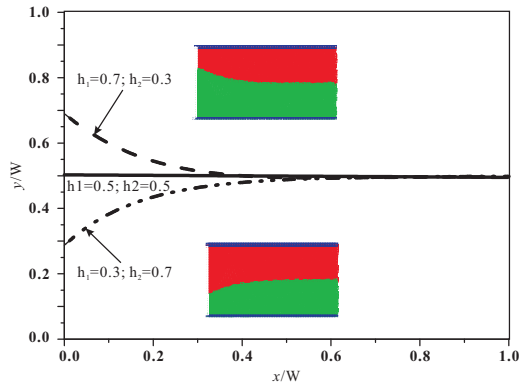

Figure 8: Evolution of interface along flow direction for liquid-liquid two-phase flow between parallel plates for different inlet velocities.

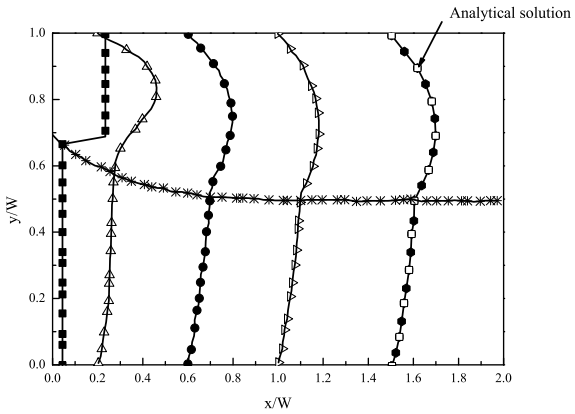

Figure 9: Evolutions of velocity and interface profiles along flow directions for $h_{1in}/\text{W}=0.7$, $\mu_1=10\mu_2$, $Q_1/Q_2=0.4185$. Symbols represent the results obtained from MPS simulations while the solid line is the results from the Level-Set Method. Symbol □ represents the analytical solution which is obtained only for the fully developed flow profile.

is $h_{1,inlet}=0.7$W. The viscosity ratio is $\mu_1/\mu_2=10$. The flow rate ratio is $Q_1/Q_2=0.4185$. The numerical result is compared with exact analytical solution of Eqs. (3.5a) and (3.5b). Thus, for liquid-liquid flow with different fluid properties, the MPS can also accurately capture the interface and velocity.

The velocity and the interface location are compared with the previous results calculated using Level-Set method. Similar as before, this figure also compared the results from MPS method with exact solutions of Eqs. (3.5a) and (3.5b). The good agreement between the MPS method, the Level-Set method and the analytical solution confirms that the MPS method can capture the evolutions of the interface under different inlet conditions.

5 Conclusions

The MPS method is used to simulate the developing procedures of liquid-liquid two-phase stratified flow between two parallel plates. This method can track fluid flow and interface deformation simultaneously without introducing any extra equations and special treatments for interface. Effects of density, viscosity and flow rate ratios are examined. The results arising from the MPS method are also compared with the Level-Set method and the exact analytical solutions. The results indicate that the MPS method can correctly capture the velocity profile and interface for liquid-liquid stratified flow.

Comparing with the level set approach, the MPS method doesn't need to define and calculate the interface. There is no additional force balance for the interface. But there are also some drawbacks for the MPS method. The particle number is constant for the fixed liquid. If the flow domain changed dramatically, the accuracy of calculation will reduce.

Furthermore, the success of the MPS method in these relatively simple flow configurations indicates that applications towards complex fluids and/or geometry is indeed promising as the method eliminates the need for an almost always otherwise necessary task of creating a mesh for the numerical solution procedure.

Acknowledgments

The authors gratefully acknowledge research support from the Agency for Science, Technology and Research (A*STAR) and Engineering Research Grant, SERC Grant No. 1021640147. T. N. Wong and Haiwang Li gratefully acknowledge research support from the Singapore Ministry of Education Academic Research Fund Tier 2. Research grant MOE 2011-T2-1-036.

Appendix A

Eq. (2.6) can be derived as:

The gradient of parameter f can be described as

$$(\nabla f)_{j-i}=\left(\frac{\Delta f}{\Delta \mathbf{r}}\right)_{j-i}. \tag{A.1}$$

In Eq. (A.1),

$$\Delta f=f_j-f_i. \tag{A.2}$$

The direction of the gradient can be described as

$$\frac{(\mathbf{r}_j-\mathbf{r}_i)}{|\mathbf{r}_j-\mathbf{r}_i|}. \tag{A.3}$$

The distance from point j to point i is

$$|\mathbf{r}_j-\mathbf{r}_i|. \tag{A.4}$$

Submitted Eqs. (A.2)-(A.4) into Eq. (A.1), the gradient of parameter f is shown

$$(\nabla f)_{j-i}=\frac{d(f_j-f_i)(\mathbf{r}_j-\mathbf{r}_i)}{|\mathbf{r}_j-\mathbf{r}_i|^2}. \tag{A.5}$$

Appendix B

Eq. (2.11) can be derived as:

The gradient of parameter f between j and i is

$$(\nabla f)_{j-i}=\frac{d[(f_j-f_i)(\mathbf{r}_j-\mathbf{r}_i)]}{|\mathbf{r}_j-\mathbf{r}_i|^2}. \tag{B.1}$$

The gradient of parameter f at point i is the total effect of neighboring particles. The effect can be described as

$$(\nabla f)_i=\frac{d}{n^0}\sum_{j\neq i}\left[\frac{f_j-f_i}{|\mathbf{r}_j-\mathbf{r}_i|^2}(\mathbf{r}_j-\mathbf{r}_i)w(|\mathbf{r}_j-\mathbf{r}_i|)\right]. \tag{B.2}$$

Eq. (2.11) in the manuscript is

$$(\nabla^2 f)_i=\nabla\cdot(\nabla f)_i. \tag{B.3}$$

Substituting Eq. (B.2) into Eq. (B.3), the Laplace operator of particle i can be expressed as

$$(\nabla\cdot(\nabla f)_{ij})_i=\frac{2d}{n^0}\sum_{j\neq i}\frac{\frac{(f_j-f_i)(\mathbf{r}_j-\mathbf{r}_i)}{|\mathbf{r}_j-\mathbf{r}_i|^2}\cdot(\mathbf{r}_j-\mathbf{r}_i)}{|\mathbf{r}_j-\mathbf{r}_i|^2}w(|\mathbf{r}_j-\mathbf{r}_i|,r_e). \tag{B.4}$$

We defined that

$$\lambda=\frac{\sum_{j\neq i}w(|\mathbf{r}_j-\mathbf{r}_i|)|\mathbf{r}_j-\mathbf{r}_i|^2}{\sum_{j\neq i}w(|\mathbf{r}_j-\mathbf{r}_i|)}. \tag{B.5}$$

Substituting Eq. (B.4) and Eq. (B.5) into Eq. (B.3), we have

$$(\nabla^2 f)_i=\frac{2d}{n^o\lambda}\sum_{j\neq i}(f_j-f_i)w(|\mathbf{r}_j-\mathbf{r}_i|). \tag{B.6}$$

Appendix C

Eq. (2.12) can be derived as:

The governing equation is:

$$\frac{D\mathbf{u}}{Dt}=-\frac{1}{\rho}\nabla p+\nu\nabla^2\mathbf{u}+\mathbf{g}. \tag{C.1}$$

The gravity effect can be ignored in the microchannel. Then Eq. (C.1) reduces into

$$\frac{D\mathbf{u}}{Dt}=-\frac{1}{\rho}\nabla p+\nu\nabla^2\mathbf{u}. \tag{C.2}$$

Eq. (C.2) can be rewritten as

$$\rho\frac{D\mathbf{u}}{Dt}=-\nabla p+\mu\nabla^2\mathbf{u}. \tag{C.3}$$

The left side of Eq. (C.1) can be rewritten as

$$\frac{D\mathbf{u}}{Dt}=\frac{\partial\mathbf{u}}{\partial t}+\mathbf{u}\cdot\nabla\mathbf{u}. \tag{C.4}$$

Substituting Eq. (C.4) into Eq. (C.3), we have

$$\rho\frac{\partial\mathbf{u}}{\partial t}+\rho\mathbf{u}\cdot\nabla\mathbf{u}=-\nabla p+\mu\nabla^2\mathbf{u}. \tag{C.5}$$

According the definition that

$$(\nabla^2 f)_i=\frac{2d}{n^o\lambda}\sum_{j\neq i}(f_j-f_i)w(|\mathbf{r}_j-\mathbf{r}_i|). \tag{C.6}$$

Eq. (C.6) can be rewritten as

$$(\nabla^2\mathbf{u})_i=\frac{2d}{n^o\lambda}\sum_{j\neq i}(\mathbf{u}_j-\mathbf{u}_i)w(|\mathbf{r}_j-\mathbf{r}_i|). \tag{C.7}$$

According the definition that

$$(\nabla f)_i = \frac{d}{n^0}\sum_{j\neq i}\left[\frac{f_j - f_i}{|\mathbf{r}_j - \mathbf{r}_i|^2}(\mathbf{r}_j - \mathbf{r}_i)w(|\mathbf{r}_j - \mathbf{r}_i|)\right]. \tag{C.8}$$

We have

$$(\nabla \mathbf{u})_i = \frac{d}{n^0}\sum_{j\neq i}\left[\frac{\mathbf{u}_j - \mathbf{u}_i}{|\mathbf{r}_j - \mathbf{r}_i|^2}(\mathbf{r}_j - \mathbf{r}_i)w(|\mathbf{r}_j - \mathbf{r}_i|)\right]. \tag{C.9}$$

Substituting Eqs. (C.7) and (C.9) into Eq. (C.5), we have

$$\begin{aligned}&\frac{mn}{\oint_{\mathrm{v}_i} w(r)d\mathrm{v}}\frac{\mathbf{u}}{\Delta t} + \mathbf{u}\frac{d}{n^0}\sum_{j\neq i}\left[\frac{\mathbf{u}_j - \mathbf{u}_i}{|\mathbf{r}_j - \mathbf{r}_i|^2}(\mathbf{r}_j - \mathbf{r}_i)w(|\mathbf{r}_j - \mathbf{r}_i|)\right]\\ =&-\nabla p + \frac{\mu_i 2d}{n^o\lambda}\sum_{j\neq i}(\mathbf{u}_j - \mathbf{u}_i)w(|\mathbf{r}_j - \mathbf{r}_i|).\end{aligned} \tag{C.10}$$

Appendix D

Eq. (C.5) can be derived as:

$$n' = n^0 - n^*. \tag{D.1}$$

The continuity equation can be described as

$$\frac{1}{\rho}\frac{d\rho}{dt} + \nabla\cdot\mathbf{u} = 0, \tag{D.2a}$$

$$\rho_i = (m\rho_n)_i = \frac{m_i n_i}{\oint_{\mathrm{v}_i} w(r)d\mathrm{v}}. \tag{D.2b}$$

Substituting the equation of the density into Eq. (D.2a), we have

$$\frac{1}{n}\frac{dn}{dt} + \nabla\cdot\mathbf{u} = 0. \tag{D.3}$$

Because that

$$\frac{1}{n^0 - n'}\frac{d(n^0 - n')}{dt} + \nabla\cdot(\mathbf{u}^0 - \mathbf{u}') = 0. \tag{D.4}$$

Comparing with the initial particle number, the derivation of particle number is small. It means that

$$n^0 \gg n'. \tag{D.5}$$

According Eq. (D.5), Eq. (D.4) reduces into

$$\frac{1}{n^0}\Big(\frac{dn^0}{dt}-\frac{dn'}{dt}\Big)+\big(\nabla\cdot\mathbf{u}^0-\nabla\cdot\mathbf{u}'\big)=0. \tag{D.6}$$

Because that

$$\frac{1}{n^0}\frac{dn^0}{dt}+\nabla\cdot\mathbf{u}^0=0. \tag{D.7}$$

We have

$$\frac{1}{n^0}\frac{dn'}{dt}+\nabla\cdot\mathbf{u}'=0. \tag{D.8}$$

Eq. (D.8) can be rewritten as

$$n'=-(\Delta t)n^0(\nabla\cdot\mathbf{u}'). \tag{D.9}$$

The modification of the velocity u' can be calculated from the pressure gradient according the simplified MAC (SMAC) method [29]:

$$\mathbf{u}'|^s=-\frac{\Delta t}{\rho}\nabla p|^{s+1}. \tag{D.10}$$

Eq. (C.4) can be rewritten as

$$\nabla p|^{s+1}=-\frac{\rho}{\Delta t}\mathbf{u}'|^s. \tag{D.11}$$

Because that

$$\nabla\cdot\nabla p|^{s+1}=-\frac{\rho}{\Delta t}(\nabla\cdot\mathbf{u}'|^s), \tag{D.12a}$$

$$\nabla^2 p|^{s+1}=-\frac{\rho}{\Delta t}(\nabla\cdot\mathbf{u}'|^s). \tag{D.12b}$$

Substituting Eq. (2.14) into Eq. (D.12b), we have

$$\big(\nabla^2 p|^{s+1}\big)_i=-\frac{\rho}{(\Delta t)^2}\frac{n'}{n^o}, \tag{D.13}$$

where $f|^s$ is the calculated value of f in step s of the iteration. Because that $n'=n^0-n^*$, Eq. (D.13) can be rewritten as

$$\big(\nabla^2 p|^{s+1}\big)_i=-\frac{\rho}{(\Delta t)^2}\frac{(n^*)_i-n^o}{n^o}. \tag{D.14}$$

References

[1] H. Gao, H. Y. Gu and L. J. Guo, Numerical study of stratified oil-water two-phase turbulent flow in a horizontal tube, Int. J. Heat Mass Tran., 46 (2003), 749–754.

[2] S. Razwan, Numerical study of stratified oil-water two phase flow in horizontal and slightly inclined pipes, in: Mech. Eng., King Fahd University of Petroleum & Minerals, 2007.

[3] C. F. Torres-Monzon, Modeling of oil-water flow in horizontal and near horizontal pipes, in: The Graduate School, The University of Tulsa, 2006.

[4] P. Vigneaux, P. Chenais and J. P. Hulin, Liquid-liquid flows in an inclined pipe, AIChE J., 34 (1988), 781–789.

[5] P. Angeli and G. F. Hewitt, Pressure gradient in horizontal liquid-liquid flows, Int. J. Multiphas Flow, 24 (1998), 1183–1203.

[6] P. Abduvayt, R. Manabe, T. Watanabe and N. Arihara, Analysis of oil/water-flow tests in horizontal, hilly terrain, and vertical pipes, SPE Production and Operations, 21 (2006), 123–133.

[7] J. Lovick and P. Angeli, Experimental studies on the dual continuous flow pattern in oil-water flows, Int. J. Multiphas Flow, 30 (2004), 139–157.

[8] A. Ullmann, M. Zamir, S. Gat and N. Brauner, Multi-holdups i n co-current stratified flow in inclined tubes, Int. J. Multiphas Flow, 29 (2003), 1565–1581.

[9] G. Oddie, H. Shi, L. J. Durlofsky, K. Aziz, B. Pfeffer and J. A. Holmes, Experimental study of two and three phase flows in large diameter inclined pipes, Int. J. Multiphas Flow, 29 (2003), 527–558.

[10] P. Angeli and G. F. Hewitt, Flow structure in horizontal oil-water flow, Int. J. Multiphas Flow, 26 (2000), 1117–1140.

[11] R. W. Lockhart and R. C. Martinelli, Proposed correlation of data for isothermal two-phase, two-component flow in pipes, Chem. Eng. Prog., 45 (1949), 39–48.

[12] M. Bentwich, Two-phase axial laminar flow in a pipe with naturally curved interface, Chem. Eng. Sci., 31 (1976), 71–76.

[13] K. B. Ranger and A. M. J. Davis, Steady pressure driven two-phase stratified laminar flow through a pipe, Can. J. Chem. Eng., 57 (1979), 688–691.

[14] N. Brauner, J. Rovinsky and D. M. Maron, Analytical solution for laminar-laminar two-phase stratified flow in circular conduits, Chem. Eng. Commun., 141-142 (1996), 103–143.

[15] A. P. A. Kurban, Stratified Liquid-Liquid Flow, in: Imperial College, University of London, London, 1997.

[16] D. Biberg and G. Halvorsen, Wall and interfacial shear stress in pressure driven two-phase laminar stratified pipe flow, Int. J. Multiphas Flow, 26 (2000), 1645–1673.

[17] A. R. W. Hall and G. F. Hewitt, Application of two-fluid analysis to laminar stratified oil-water flows, Int. J. Multiphas Flow, 19 (1993), 711–717.

[18] S. H. Khor, M. A. Mendes-Tatsis and G. F. Hewitt, One-dimensional modelling of phase holdups in three-phase stratified flow, Int. J. Multiphas Flow, 23 (1997), 885–897.

[19] G. K. Elseth, H. K. and M. C. Melaaen, Measurement of velocity and phase fraction in stratified oil/water flow, Int. Symp. Multiphase Flow Trans. Phenomena, (2000), 206–210.

[20] Y. F. Yap, J. C. Chai, K. C. Toh, T. N. Wong and Y. C. Lam, Numerical modeling of unidirectional stratified flow with and without phase change, Int. J. Heat Mass Tran., 48 (2005), 477–486.

[21] T. Coupez, Metric construction by length distribution tensor and edge based error for anisotropic adaptive meshing, J. Comput. Phys., 230 (2011), 2391–2405.

[22] T. Coupez, G. Jannoun, N. Nassif, H. C. Nguyen, H. Digonnet and E. Hachem, Adaptive time-step with anisotropic meshing for incompressible flows, J. Comput. Phys., 241 (2013), 195–211.
[23] C. H. Oh, Interfaical interaction in two-phase gas-non-Newtonian liquid flow systems, in: Department of Chemical Engineering, Washington State University, Washington, 1985, pp. 254.
[24] D. Barnea, O. Shoham, Y. Taitel and A. E. Dukler, Flow pattern transition for gas-liquid flow in horizontal and inclined pipes. Comparison of experimental data with theory, Int. J. Multiphas Flow, 6 (1980), 217–225.
[25] D. L. Schubring, Behavior Interrelationships in Annular Flow, in University of Wisconsin-Madison, Madison, Wisconsin, 2009.
[26] S. Koshizuka and Y. Oka, Moving-particle semi-implicit method for fragmentation of incompressible fluid, Nucl. Sci. Eng., 123 (1996), 421–434.
[27] H. Gotoh and T. Sakai, Key issues in the particle method for computation of wave breaking, Coast Eng., 53 (2006), 171–179.
[28] S. Koshizuka, A. Nobe and Y. Oka, Numerical analysis of breaking waves using the moving particle semi-implicit method, Int. J. Numer. Meth. Fl., 26 (1998), 751–769.
[29] F. H. H. Anthony and A. Amsden, The SMAC Method: A Numerical Technique for Calculating Incompressible Fluid Flows, Los Alamos Scientific Laboratory of the University of California, 1970.